Heliyon 9 (2023) e15431

Contents lists available at ScienceDirect

Heliyon

journal homepage: www.cell.com/heliyon

Research article

Design and synthesis of novel bis-pyridinium based-ionic liquids as potent antiparasitic agents

Esraa Abdelhamid Moneer [a], Basant A. Bakr [b], Sara H. Akl [a], Yahya H. Shahin [a], Bassma H. Elwakil [a,*], Mohamed Hagar [c], Keshav Raj Paudel [d], Ateyatallah Aljuhani [e], Mohamed Reda Aouad [e], Nadjet Rezki [e]

[a] Department of Medical Laboratory Technology, Faculty of Applied Health Sciences Technology, Pharos University in Alexandria, Alexandria, Egypt
[b] Department of Zoology, Faculty of Science, Alexandria University, Alexandria, 21321, Egypt
[c] Department of Chemistry, Faculty of Science, Alexandria University, Alexandria, 21321, Egypt
[d] Department of Oriental Medicine Resources, Mokpo National University, Muan-gun, Jeonnam, 58554, Republic of Korea
[e] Department of Chemistry, College of Science, Taibah University, Al-Madinah Al-Munawarah, 30002, Saudi Arabia

ARTICLE INFO

Keywords:
Ionic liquids
Dicationic ionic liquids
Toxoplasmosis infections
Antiparasitic agents

ABSTRACT

Focused bis-pyridinium based-ionic liquids were successfully synthesized through the quaternization of the selected 1,2-di(pyridin-4-yl)ethane followed by metathetical anion exchange. The synthesized pyridinium derivatives were fully characterized using various NMR-spectroscopic techniques including ^{1}H, ^{13}C, ^{11}B, ^{31}P and ^{19}F NMR. The synthesized compounds were tested for their potential effect against *Toxoplasma gondii*. It was revealed that compound 5 had higher antiparasitic activity compared to other compounds. Parasitic reduction percentage reached 38, 50, 77 and 79 for groups III, IV, V and VI respectively in the liver with noticed distortion and deformation in tachyzoites' shape. Surprisingly there was no statistically significant difference between the synthesized compound 5 and the known anti-toxoplasmosis drug pyrimethamine. Histopathological study proved the effectiveness of the synthesized compound 5 on liver, spleen and brain tissues with observed better histological features compared to pyrimethamine treated group. The present investigation may pave the way to the possible use of compound 5 to replace the known drug pyrimethamine with better antiparasitic profile and fewer side effects.

1. Introduction

For many years, ionic liquids (ILs), which are essentially 'liquid salts' based on organic and/or inorganic ions and may encompass more than one cation or anion, were known as salts that melt at temperatures around 100 °C [1,2] These are common class of bis-ionic liquids (bis-ILs) that contain a bis-cations and two identical anions, known as di-cationic ionic liquids, and have emerged as an intriguing and entertaining modern material in technology and science due to their broad range of uses in a variety of fields [3]. The chemistry of ILs has recently get to be a contentious issue, as it is critical in the design and build out of modern scaffolds, along with understanding their biological benefits and attributes that aid in their development and synthesis [1,4,5]. These tunable molecules are well known for their high stability and safety properties, which include nonvolatility and nonflammability, negligible vapor pressure, thermal stability and high ionic conductivity, easy recyclability, and high miscibility in both organic and aqueous solvents. They are

* Corresponding author.
E-mail address: Bassma.hassan@pua.edu.eg (B.H. Elwakil).

https://doi.org/10.1016/j.heliyon.2023.e15431
Received 11 January 2023; Received in revised form 24 March 2023; Accepted 7 April 2023
Available online 14 April 2023

easily designed and constructed by combining bulky organic cations with either inorganic or organic anions to achieve the desired structural frameworks with focused characteristics like melting point, lower toxicity, and density, as well as continuing to increase benefits in biological implantation [6–12].

Toxoplasmosis is a zoonotic infection that causes a distinct health problem in humans, wildlife, and domestic animals. It can infect animals and humans in any ecosystem, including food, soil, and water [13]. *Toxoplasma gondii* is considered among the most widely distributed parasites. Nearly one-third of the world's population was exposed to *T. gondii* through contaminated food and water, especially in areas with poor sanitation [14]. It is also considered a global health risk due to its high global seroprevalence, which varies with various regional differences in hygiene, diet, habits, climate, and host susceptibility [15].

It has been reported that *T. gondii* spreads by three main routes, the first is by eating oocysts in contaminated water, soil, or food; the second is by ingesting cysts from infected animal tissues; it is due to vertical transmission from HIV to the fetus [13]. Infection is usually considered asymptomatic if it has no symptoms. Primary infections can harm the fetus during pregnancy and even lead to abortion. Moreover, in immunocompromised humans and animals, primary parasitic infection or relapse can lead to severe neurological clinical manifestations, with implications for public health and animal production [16]. When infection first begins, *T. gondii* spreads to mesenteric lymph nodes before invading blood and lymphatic vessels to spread to other organ systems. The parasite can then grow almost anywhere in the body's cells. Similar to many other common explicitly require intracellular pathogenic microbes, *T. gondii* infection triggers a type 1 polar immune response that targets both innate and adaptive immunity [13]. It is well recognized that the production of pro-inflammatory cytokines interferes with the host's main defense mechanism against toxoplasmosis [17]. Tachyzoite replication is squelched by the host's T-cell mediated immune responses, which may result in chronic infection or parasite clearance [18]. Since 1950, sulfadiazine and pyrimethamine have been used in combination to treat human toxoplasmosis infections. Through simultaneous inhibition of the enzymes dihydrofolate reductase and dihydropteroate synthase, these medications work to prevent the synthesis of folate (essential enzymes for parasite replication and survival) [19,20]. Although, Sulfadiazine exhibits many side effects and might lead to megaloblastic anemia, granulocytopenia and leukopenia [19]. Besides that, pyrimethamine is highly harmful because it encounters the host's and parasite's biochemical pathways in overall [21].

These attributes have improved dramatically our both functional and structural experience and knowledge as part of our current advancement for the development of powerful and effective ionic liquids framework carrying di-pyridinium ionic liquids [22–25]. Many research groups have engaged in a broad array of novel chemical development against *T. gondii* to find anti-toxoplasmosis drugs that are extremely effective and have minimal risky side effects. Thus, in this study, we have anticipated to design, synthesize and characterize focused bis-pyridinium ionic liquids encompassing benzyl side chains and different counter-anions. Furthermore, we investigated the antiparasitic properties of the synthesized bis-ILs against Toxoplasmosis, establishing their reduction activity. Premised on a thorough literature review, this study is the first to investigate the potential of bis-ILs to attenuate the *anti-T. gondii* infection.

2. Experimental

2.1. Chemistry

2.1.1. General methods

The melting points were measured using a Stuart Scientific SMP1 instrument and are uncorrected. The characterization of the newly designed bis-pyridinium ionic liquids has been achieved by IR, ^{1}H, ^{13}C, ^{19}F, ^{31}P, ^{11}B-NMR spectroscopy and elemental analysis. The 500 MHz Jeol NMR spectrometer was used to elaborate all NMR spectra. Elemental analyzes were performed using a GmbH-Vario EL III Elemental Analyzer.

2.2. Synthesis and characterization of 4,4'-(ethane-1,2-diyl)bis(1-benzylpyridin-1-ium) bromide (2)

Under stirring, benzyl bromide (20 mmol) was dropwise added to 1,2-di(pyridin-4-yl)ethane (**1**) solution (20 mmol) in acetonitrile (40 mL). TLC showed that the starting material had been consumed after 16 h heating under reflux. Evaporation under reduced pressure was used to reduce the solvent. The resulting product was filtered to yield the desired di-cationic pyridinium ionic liquid **2**.

Yield: 94%; mp: 35–36 °C. IR (υ, cm^{-1}): 3052 (Sp^{2}C–H), 2988 (Sp^{3}C–H), 1630 (C═N), 1564 (C═C).^{1}H NMR (DMSO-d_6, 400 MHz): δ_H = 9.18 (2H, s, Pyridyl-**H**), 8.14 (2H, s, Pyridyl-**H**), 7.50 (2H, s, Ph-**H**), 7.34 (3H, d, J = 4.0 Hz, Ph-**H**), 5.83 (2H, s, NC**H**$_2$), 3.23 (2H, s, CH$_2$C**H**$_2$). ^{13}C NMR (DMSO-d_6, 100 MHz): δ_C = 161.22, 144.70, 134.90, 129.85, 129.72, 129.29, 128.73 (**C**═N, Ar-**C**); 62.83 (N**C**H$_2$); 34.28 (CH$_2$**C**H$_2$). Calculated for $C_{26}H_{26}Br_2N_2$: C, 59.33; H, 4.98; N, 5.32. Found: C, 59.56; H, 4.87; N, 5.49.

2.3. General metathesis procedure for the synthesis of bis-benzyl pyridinium based-ionic liquids 3-5

A stirred suspension of compound **2** (1 mmol) in acetonitrile (20 mL) containing the corresponding potassium hexafluorophosphate, sodium tetrafluoroborate, and/or sodium thiocyanate (2.2 mmol) was refluxed for 24 h. After the mixture cooling, the resulting crude product was collected using filtration, which was then washed with acetonitrile, left to dry and crystallized from ethanol yielding the targeted dicationic bis-pyridinium derivatives **3**–**5**.

2.4. Characterization of 4,4'-(ethane-1,2-diyl)bis(1-benzylpyridin-1-ium) hexafluorophosphate (3)

Yield: 90%; syrup. IR (υ, cm^{-1}): 3047 (Sp^2C–H), 2997 (Sp^3C–H), 1636 (C═N), 1570 (C═C).^{1}H NMR (DMSO-d_6, 400 MHz): δ_H = 9.16 (2H, s, Pyridyl-**H**), 8.11 (2H, s, Pyridyl-**H**), 7.51 (2H, s, Ph-**H**),7.36 (3H, d, J = 4.0 Hz, Ph-**H**), 5.82 (2H, s, NC**H**$_2$), 3.27 (2H, s, $CH_2C\mathbf{H}_2$). ^{13}C NMR (DMSO-d_6, 400 MHz): δ_C = 161.20, 144.67, 134.91, 129.85, 129.89, 129.31, 128.69 (**C**═N, Ar-**C**); 62.86 (N**C**H$_2$); 34.30 ($CH_2\mathbf{C}H_2$). ^{31}P NMR (DMSO-d_6, 162 MHz) δ_P = -131.01 to-157.36 (1P, sept, **P**F$_6$). ^{19}F NMR (DMSO-d_6, 377 MHz): δ_F = −69.25 (6F, d, P**F$_6$**). Calculated for $C_{26}H_{26}F_{12}N_2P_2$: C, 47.57; H, 3.99; N, 4.27. Found: C, 47.30; H, 3.88; N, 4.44.

2.5. Characterization of 4,4'-(ethane-1,2-diyl)bis(1-benzylpyridin-1-ium) tetrafluoroborate (4)

Yield: 92%; syrup. IR (υ, cm^{-1}): 3049 (Sp^2C–H), 2999 (Sp^3C–H), 1638 (C═N), 1573 (C═C).^{1}H NMR (DMSO-d_6, 400 MHz): δ_H = 9.10 (2H, d, J = 4.0 Hz, Pyridyl-**H**), 8.07(2H, d, J = 4.0 Hz, Pyridyl-**H**), 7.48–7.39 (5H, m, Ph-**H**), 5.76 (2H, s, NC**H**$_2$), 3.27 (2H, s, $CH_2C\mathbf{H}_2$). ^{13}C NMR (DMSO-d_6, 100 MHz): δ_C = 161.10, 144.83, 134.95, 129.88, 129.78, 129.21, 128.66 (**C**═N, Ar-**C**); 63.22 (N**C**H$_2$); 34.27 ($CH_2\mathbf{C}H_2$). ^{11}B-NMR (DMSO-d_6, 128 MHz): δ_B = −1.28 to −1.30 (1B, m, **B**F$_4$). ^{19}F NMR (DMSO-d_6, 377 MHz): δ_F = −148.24, −148.31 (4F, 2d, B**F**$_4$). Calculated for $C_{26}H_{26}B_2F_8N_2$: C, 57.82; H, 4.85; N, 5.19. Found: C, 57.61; H, 4.95; N, 5.32.

2.6. Characterization of 4,4'-(ethane-1,2-diyl)bis(1-benzylpyridin-1-ium) thiocyanate (5)

Yield: 90%; mp: 47–48 °C. IR (υ, cm^{-1}): 3043 (Sp^2C–H), 2980 (Sp^3C–H), 2064 (SCN), 1634 (C═N), 1570 (C═C). ^{1}H NMR (DMSO-d_6, 400 MHz): δ_H = 9.21 (2H, s, Pyridyl-**H**), 8.15 (2H, s, Pyridyl-**H**), 7.53 (2H, s, Ph-**H**), 7.38 (3H, s, Ph-**H**), 5.85 (2H, s, NC**H**$_2$), 3.29 (2H, s, $CH_2C\mathbf{H}_2$). ^{13}C NMR (DMSO-d_6, 100 MHz): δ_C = 161.22, 144.79, 134.96, 129.87, 129.76, 129.26, 128.69 (**C**═N, Ar-**C**); 63.10 (N**C**H$_2$); 34.29 ($CH_2\mathbf{C}H_2$). Calculated for $C_{28}H_{26}N_4S_2$: C, 69.68; H, 5.43; N, 11.61. Found: C, 69.85; H, 5.36; N, 11.73.

2.7. Cytotoxicity test

Cytotoxicity test was determined in a liver cell line (HepG2). 100 units/mL of penicillin and 100 mg/mL of streptomycin were added to DMEM medium (supplemented with 10% FBS) to grow the normal liver cells which were maintained in 5% CO_2 at 37 °C. Then two-fold serially diluted concentrations of each tested compound were prepared. Confluent monolayers of normal liver cells were grown in 96-well microtiter plates for 24 h then the prepared concentrations were added to the grown cells then furtherly incubated for 72 h. After the incubation period, 20 μL MTT (5 mg/mL) was added to each well, incubated at 37 °C for 4 h. The optical density (OD) was measured at 570 nm and the cytotoxic concentration (CC_{50}), was estimated from graphic plots of the dose response curve for each tested concentration [26].

2.8. Parasite

The virulent strain *T. gondii* RH was supplied from the Parasitology Laboratory of Theodor Bilharz Research Institute, Giza, Egypt. The parasite was kept alive at Pharos University (Alexandria) by serial intraperitoneal passages of tachyzoites in Swiss albino mice. Peritoneal fluid was washed using phosphate-buffered saline (PBS). A drop of the collected peritoneal exudate was counted using hemocytometer and mice were infected with specified number of tachyzoites (2500 tachyzoites/100 μL).

2.8.1. Drugs preparation

The tested Di-ILs **2, 4** and **5** were suspended in saline (100 μL) and orally administered as a single dose/mouse for 7 days starting from the day of infection.

2.8.2. Animal grouping and experimental design

The study here included 60 BALB/c male mice (6–8 weeks old) weighing between 20 and 25 g. Mice were divided into 6 groups (10 mice/group) in which each mouse was assigned to specified treatment regimen (received via oral gavage needle starting from the day of infection) as following:

Group I: Healthy control group (received 100 μL saline for 7 days).

Group II: Infected untreated control group (received 100 μL of saline for 7 days).

Group III: Infected, compound **2** treated group (received 100 μL of compound **2** at a dose of 12.5 mg/kg/day for 7 days).

Group IV: Infected, compound **4** treated group (received 100 μL of compound **4** at a dose of 12.5 mg/kg/day for 7 days).

Group V: Infected, compound **5** treated group (received 100 μL of compound **5** at a dose of 12.5 mg/kg/day for 7 days).

Group VI: Infected, pyrimethamine treated group (received 100 μL of pyrimethamine at a dose of 12.5 mg/kg/day for 7 days).

Each mouse was intraperitoneally infected with RH strain at a dose of 2500 tachyzoites/100 μL except the healthy control group. All the tested drug doses were fixed as described for the control known drug pyrimethamine (12.5 mg/kg/day for 7 days) according to Romand et al. [27]; Jiang et al. [28] and Jafari et al. [29].

Evaluation of the treatment efficacy:

2.8.3. Parasitological study

2.8.3.1. Survival time. Survival time was assessed daily for each assigned group for 30 days and Kaplan-Meier survival curve was used to determine the percentage of mice living over time [30].

2.8.3.2. Estimation of the parasite count. On day 8, mice were anesthetized and sacrificed by cervical dislocation. Peritoneal exudate, liver, spleen, and brain tissue were collected from all assigned groups to assess the tachyzoites count. A thin smear was prepared from each sample, fixed with methanol, then dried and stained with Giemsa stain for 10 min. After staining the prepared slides were washed with tap water drop wisely. 10 different fields were examined using light microscope (oil immersion lens) to measure the mean parasite count in each subgroup (ten fields/each slide and three slides/each organ) [31,32]. Then parasite percent reduction (%R) was calculated through the following formula:

Where %R represents percent reduction, C represents the number of tachyzoites in the control group (untreated group), and E represents the number of tachyzoites in the study group of mice [33].

2.8.4. Morphological study of tachyzoites of T. gondii

On day 8, the peritoneal fluid of all infected treated subgroups was collected, followed by fixation in glutaraldehyde, then prepared for scanning electron microscope (SEM) examination of the tachyzoites' ultrastructure [34].

2.9. Histopathological study

Liver, spleen, and brain tissues were taken from each mouse at the end of the study, followed by fixation step in 10% formalin, paraffinized, sectioned, then stained with hematoxylin-eosin (H&E), and finally examined by light microscopy for possible histopathological changes [34].

2.10. Statistical analysis

The data was displayed as mean SD. SPSS version 20 was used to analyze the data. The ANOVA F-test was employed to calculate the difference in numerical variables between groups.

3. Results and discussion

3.1. Chemistry

Ionic liquids are usually prepared by quaternization of nitrogen-containing molecules. In this study, the focused 1,2-di(pyridin-4-yl)ethane (**1**) was selected as the starting reactant for the production of the desired bis-ionic liquids (bis-ILs), as shown in Scheme 1. Thereby, the two pyridine nitrogen atoms of the dipyridylethane (**1**) were bis-alkylated with two equivalents of benzyl bromide in refluxing acetonitrile, yielding the bis-benzyl pyridinium bromide in high yield (94%) (Scheme 1).

The ^{1}H and ^{13}C NMR data of compound **2** supported the accomplishment of this quaternization procedure. Therefore, the proton NMR spectrum showed the appearance of two distinct singlets at δ_H 5.83 and 3.23 ppm of 1:1 ratio that can be assigned to the benzylic N**C**H$_2$ and C**H**$_2$CH$_2$ protons, respectively. The carbon signals belonging to the same groups N**C**H$_2$Ph and **C**H$_2$CH$_2$ resonated in its ^{13}C NMR spectrum at 62.83 and 34.28 ppm, respectively (See experimental section). These results confirmed the presence of two benzyl groups in its structure.

The bis-pyridinium ionic liquid bromide **2** was then metathetically treated to displace the two bromide atoms and insert new counter anions (PF_6^-, BF_4^-, NCS^-). In this regard, thermal treatment of bis-ILs **2**, in acetonitrile for 24 h, with various metal salts afforded the corresponding bis-pyridinium ionic derivatives **3**–**5** tethering such desired counter anions in 90–92% yields.

The metathesis reaction was successful, as evidenced by spectroscopic analysis of the resulting ILs **3**–**5**. However, their ^{1}H and ^{13}C

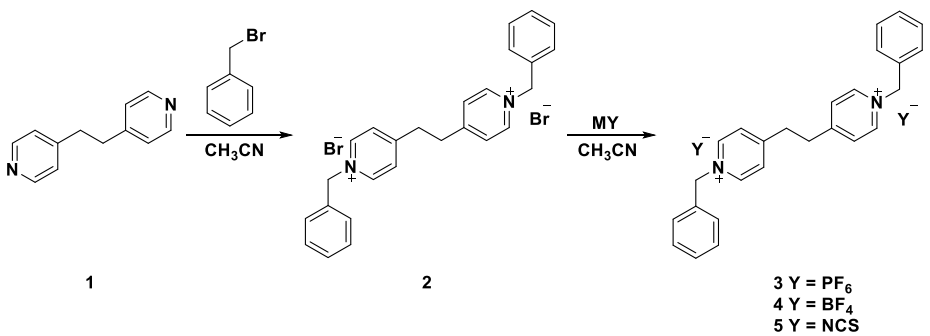

Scheme 1. Synthesis of bis-benzyl pyridinium based-ionic liquids **2**–**5.**

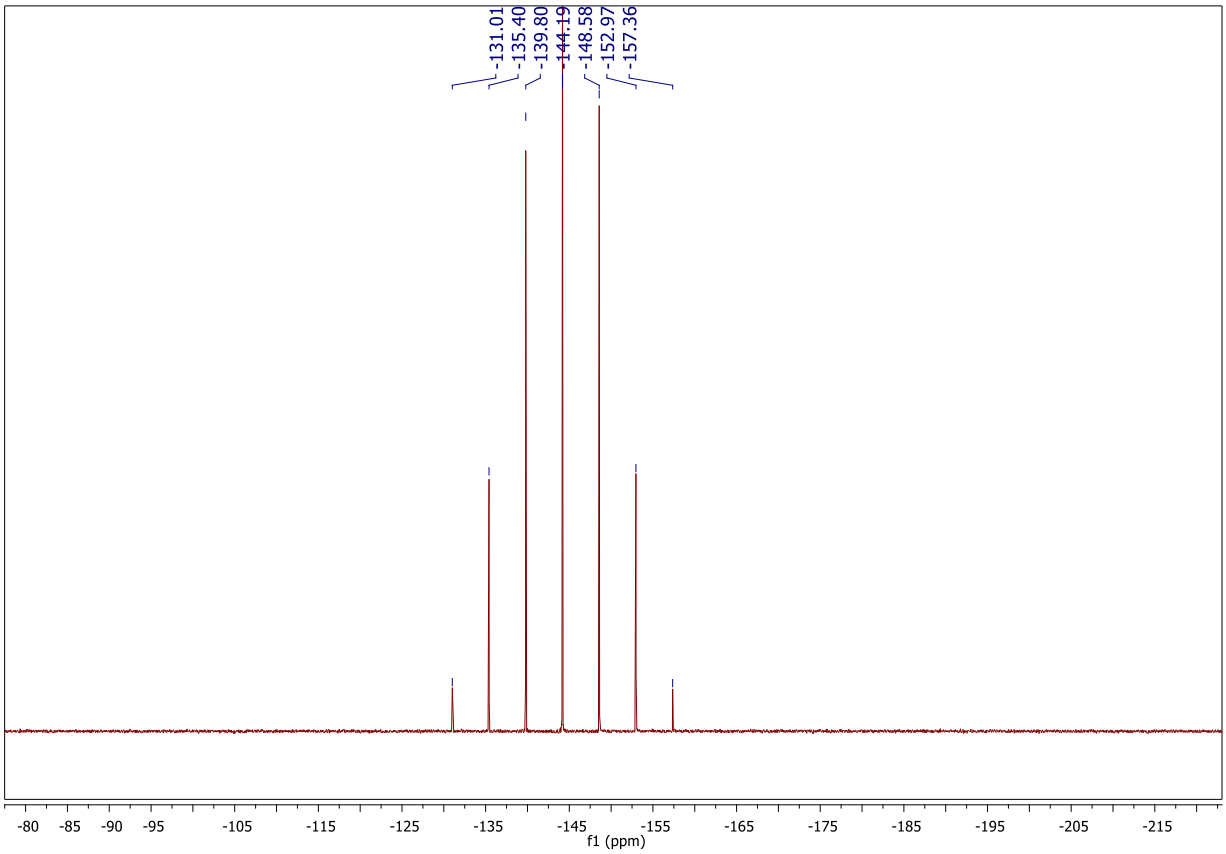

Fig. 1. ^{31}P NMR spectrum of compound **3**.

NMR spectra did not differ from those of the corresponding bromide analogue **2**.

The incorporation of two PF_6^- anions on the structure of derivative **3** was thus proved by the investigation of the ^{31}P and ^{19}F NMR spectra. The ^{19}F NMR spectrum (Fig. 1) disclosed one distinct doublet at −69.25 ppm, whereas the ^{31}P spectrum (Fig. 2) has been characterized by one septet between −131.01 and −157.36 ppm.

The presence of one distinct doublet at −69.25 ppm was detected in the ^{19}F NMR spectrum (Fig. 1), whereas one septet was detected in the ^{31}P spectrum between −131.01 and −157.36 ppm (Fig. 2).

The ^{11}B NMR and ^{19}F NMR analysis of the resulted di-pyridinium **4** facilitated the confirmation of the tetrafluroborate (BF_4^-) anion exchange. The boron spectrum (Fig. 3) showed a characteristic multiplot between −1.28 and −1.30 ppm, and the ^{19}F NMR spectrum (Fig. 4) displayed two doublets at −148.24 and −148.30 ppm.

In contrast to compounds **3** and **4**, IR spectroscopy proved to be very useful in confirming the formation of di-cationic ionic liquid **5** with thiocyanate (NCS^-) as counter anions due to the appearance of a strong absorption band at 2065 cm^{-1} attributed to such an anion (Fig. 5).

3.2. Cytotoxicity study

The in vitro cytotoxic effect of the synthesized compounds was evaluated in HepG2 cell line. It was revealed that at 500 μg/mL of the tested compounds 3, 4 and 5, the normal liver cell viability% was 19.4, 30.1 and 37.14% respectively (Fig. 6). Moreover, data revealed that compound 5 showed the highest cell viability% among the tested compounds with CC_{50} reached 375 μg/mL.

3.3. Antiparasitic activity

3.3.1. Survival rate

The survival rate was studied among the assigned groups for 30 days and data revealed that Group I (healthy uninfected mice) showed the highest mean survival time compared to infected groups. It was noticed that among the infected treated groups, Group V and VI showed the highest survival time (Fig. 7).

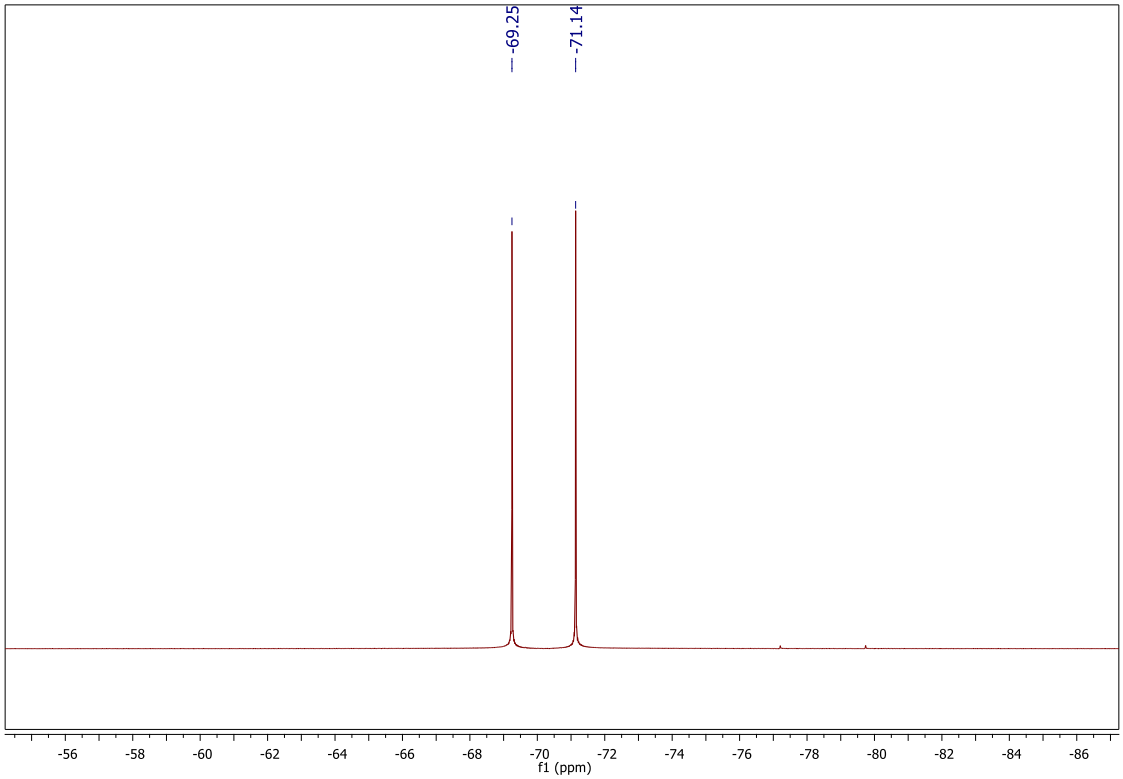

Fig. 2. ^{19}F NMR spectrum of compound **3**.

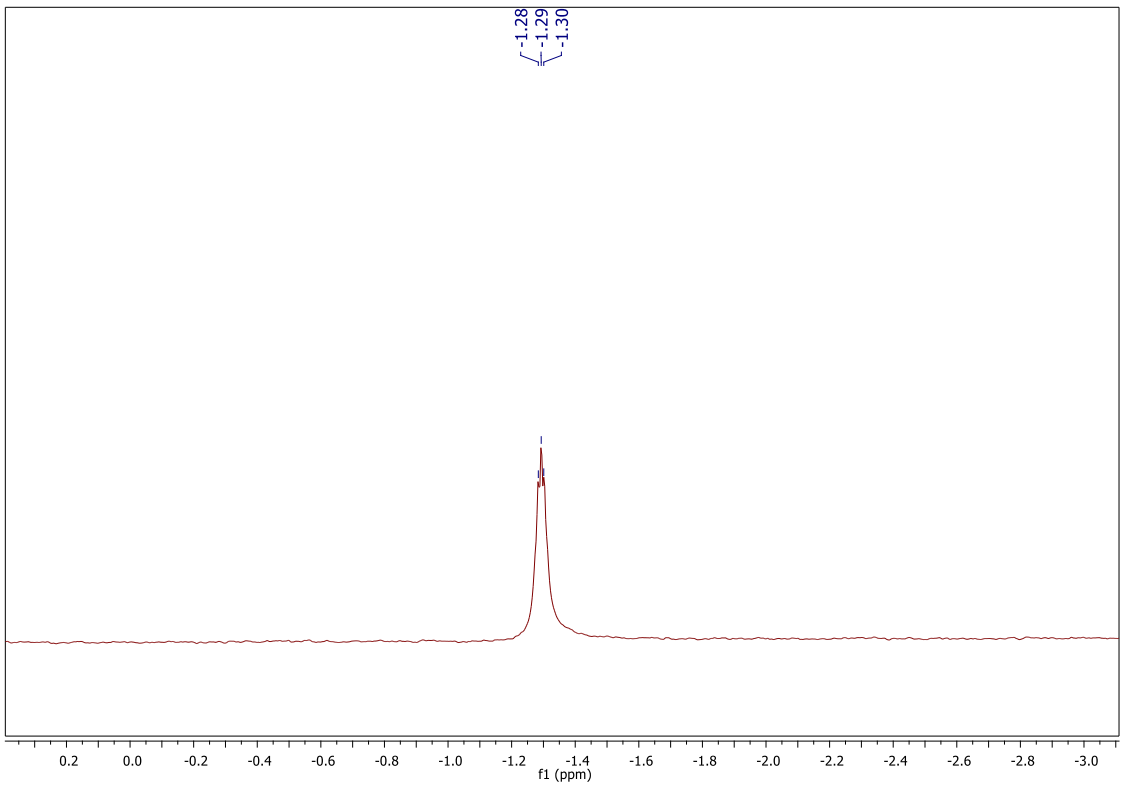

Fig. 3. ^{11}B-NMR spectrum of compound **4**.

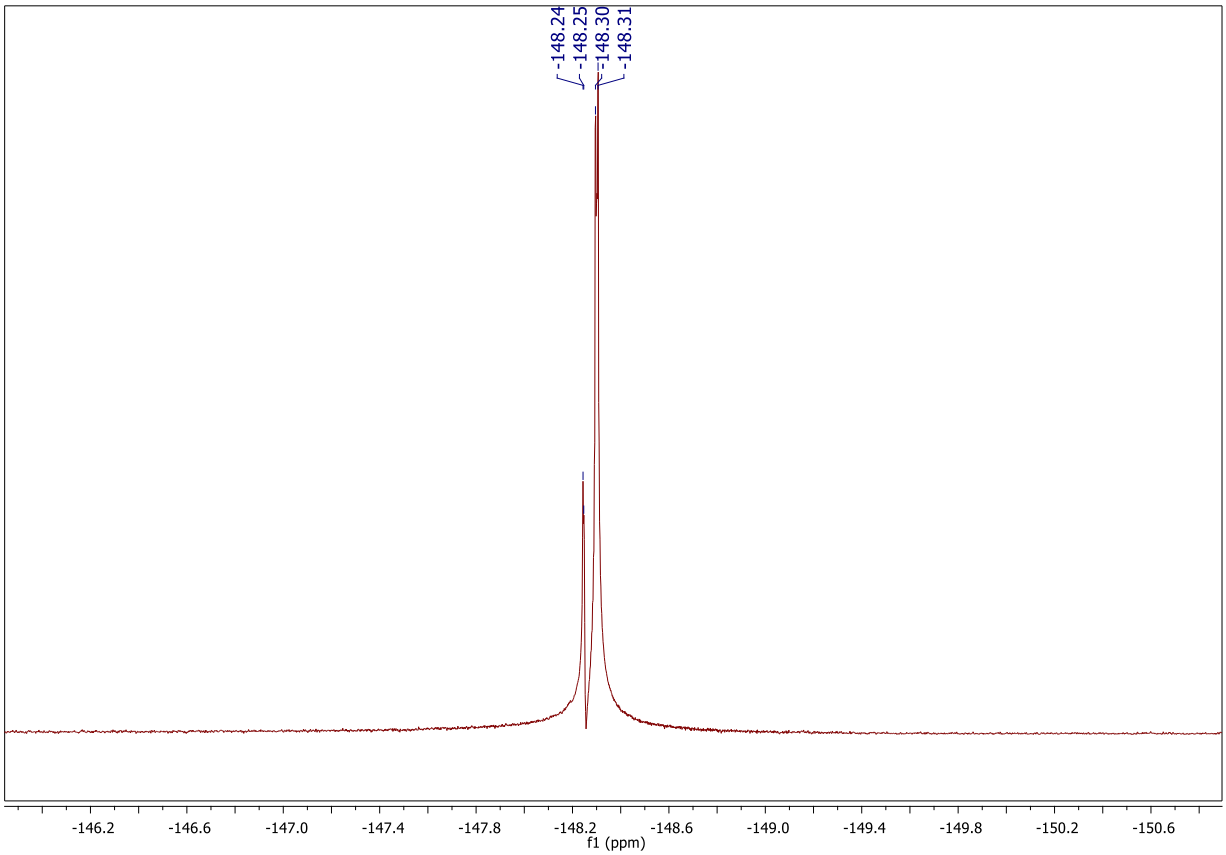

Fig. 4. ^{19}F NMR spectrum of compound **4**.

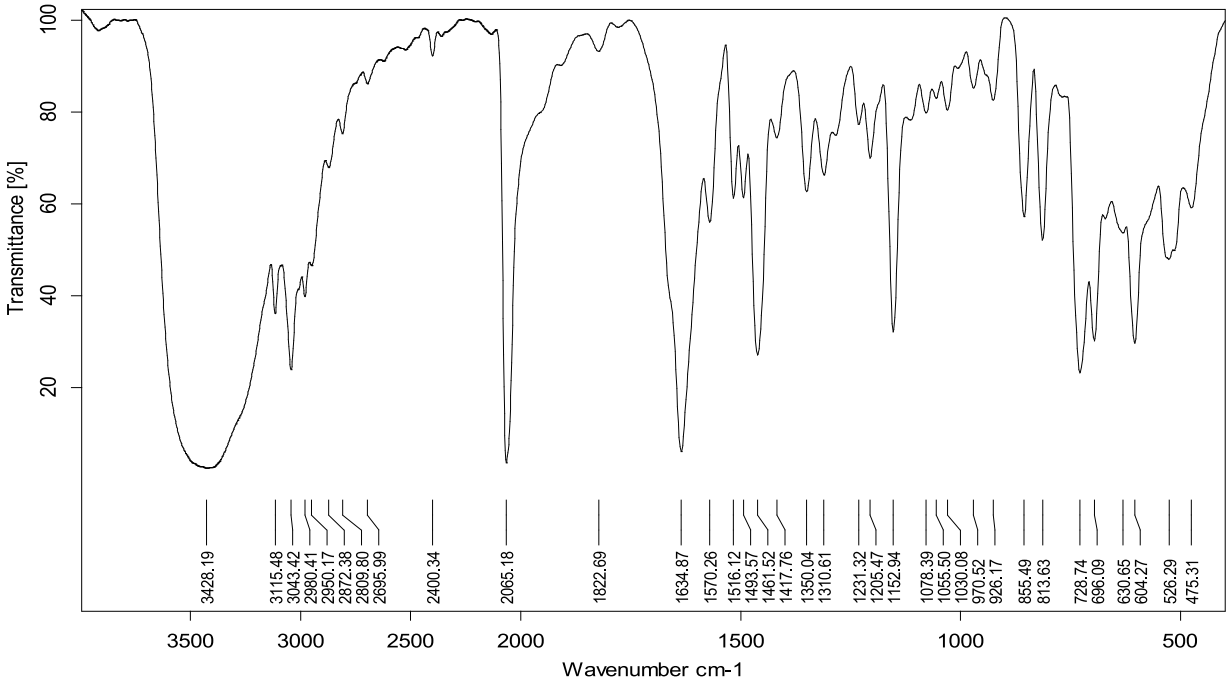

Fig. 5. IR spectrum of compound **5**.

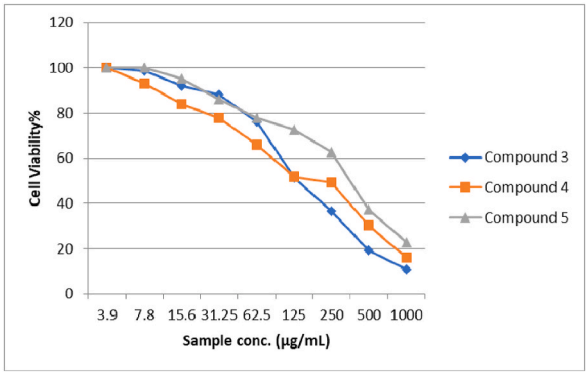

Fig. 6. Cytotoxic effect of the synthesized compounds.

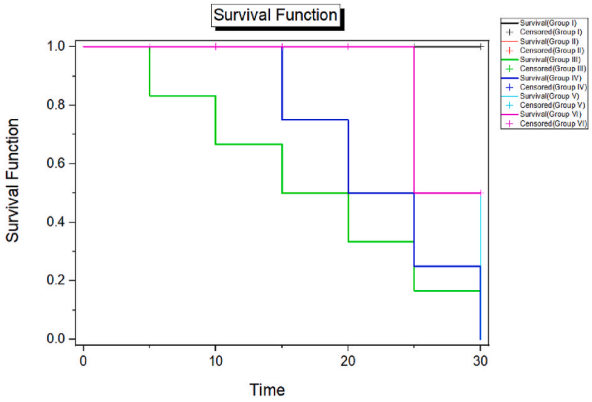

Fig. 7. Kaplan-Meier overall survival curve of the tested groups.

Table 1
Number and rate of reduction of parasites in organs of RH-infected mice.

	Liver (n = 10)	Spleen (n = 10)	Brain (n = 10)
Group II[a]			
Mean ± SD	14.9 ± 1.45[b,c,d,e]	8.9 ± 1.37[b,c,d,e]	1.4 ± 0.66[c, e]
Group III (IL 2)[b]			
Mean ± SD	9.3 ± 1.95[a,c,d,e]	7.2 ± 1.32[a,c,d,e]	1.1 ± 0.54[c,e]
R%	38	19	21
Group IV(IL 3)[c]			
Mean ± SD	7.4 ± 1.78[a,b,c,e]	5.4 ± 0.97[a,b,c,e]	0.8 ± 0.60[e]
R%	50	39	43
Group V (IL 5)[d]			
Mean ± SD	3.5 ± 0.53[a,b,d]	2.8 ± 0.63[a,b,d]	0.3 ± 0.46[a,b]
R%	77	69	79
Group VI(pyrimethamine)[e]			
Mean ± SD	3.2 ± 0.79[a,b,d]	2.5 ± 0.71[a,b,d]	0.2 ± 0.40[a,b,d]
R4%	79	72	86
F *p*	116.11	70.37	8.11
	<0.001	<0.001	<0.001

n: The number of mice in the subgroup; **SD**: standard deviation, F: F test (ANOVA) and $p \leq 0.05$(statistically significant). [a]Significant with subgroup **II**; [b]Significant with subgroup **III**; [c]Significant with subgroup **IV**; [d]Significant with subgroup **V**; [e]Significant with subgroup **VI**.

3.3.2. Parasite count and percent reduction (%R)

Mean tachyzoite counts were significantly high in all the experimental groups in relation to the liver impression smears compared to other organs with %R reached 38, 50, 77 and 79 for groups III, IV, V and VI respectively with statistically significant differences with untreated infected group (group II).

Statistically significant reductions in tachyzoites count and the highest rate of reduction among the treated mice was recorded in groups **V** and **VI** in all organs compared to untreated infected group. However, there was no statistically significant difference between these two groups (group V and VI) (Table 1, Fig. 8 (1–3))

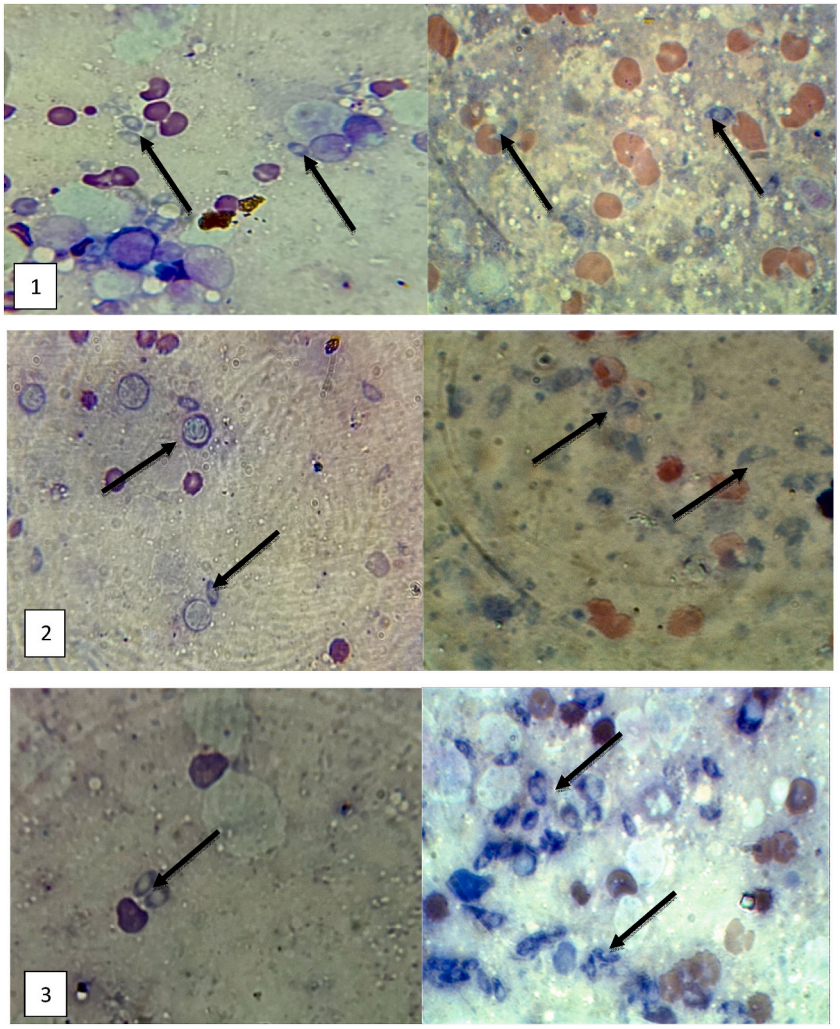

Fig. 8. Tachyzoites of T. gondii of infected mice which received compound **5** in Giemsa-stained liver tissue (**1**), Spleen (**2**) and brain (**3**) impression smears, X 1000.

Di-cationic and similar compounds that use amidine groups as the source of the cationic moiety have been tested for their antimicrobial effects and their actions against a variety of human pathogens, including *Toxoplasma gondii*, which may approve our findings [35]. Furthermore, a previous study that aimed to evaluate the rate of growth of *T. gondii* tachyzoites in Human Foreskin Fibroblast (HFF) cell line using two in vitro techniques revealed that 2-pyridine bearing 5-substituted 4-thiazolidinone and 2-pyridinyl hydrazinyl derivatives, exhibited the best *anti-T. gondii* activities with low cytotoxicity [36]. Moreover, Hopper et al. [37] discovered that 5-(4-(3-(2-methoxypyrimidin-5-yl)phenyl)piperazin-1-yl)pyrimidine-2,4-diamine was extremely effective in regulating the active infection of the hypervirulent strain of *T. gondii* in the murine model.

Scanning electron microscope study of the control group (II) revealed a normal smooth surface of *T. gondii* tachyzoites while SEM analysis of group V peritoneal fluid showed distortion and deformation in tachyzoites' shape (Fig. 9 (A-C)).

3.4. Histopathological study

3.4.1. Liver

The findings indicate normal cytoarchitecture of hepatocytes going to extend from the central vein, which was confirmed by plate 1 of the control group and groups **III** and **VI** illustrating treatment effectiveness in contrast to antibiotic effects. A clogged, dilated central vein was also seen in the negative control group.

Furthermore, in groups, normal cells in the Center had polyhedral shape, vacuolated acidophilic cytoplasm, and rounded vesicular nuclei (1, 3, and 6). The tested compound **2** group has increased vacuolation, indicating that therapy had the least effect on those hepatocytes. Hepatic sinusoids were observed to be tiny spaces surrounded by flattened endothelial cells. In way of comparison to this description, the negative control group, groups **IV**, **V**, and **VI** showed congestion of blood sinusoids, with group **V** showing a decrease

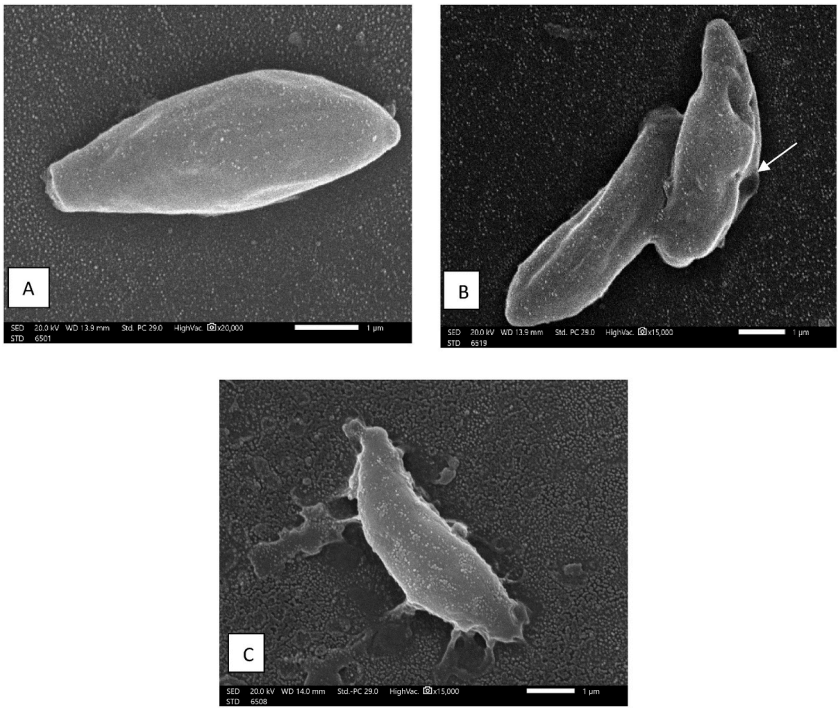

Fig. 9. SEM photo of tachyzoite of *Toxoplasma gondii* in infected unreeled drug group showing regular smooth surface and evident conoid (x 20,000) (A) while (B, C) showing *Toxoplasma gondii* tachyzoite in group V which shows irregular, ridge surface and irregular papules and dimples (arrow) (x 15,000).

in congestion, indicating that the investigated derivative **5** had a greater effect on liver tissue. Normal scattered irregular kupffer cells with oval nuclei between the hepatic cords in all groups.

Early apoptotic symptoms including such hazy vacuolated cytoplasm and imprecise cell borders were noticed in the negative control group. Nuclear alterations include nuclear division, nuclear eccentricity, and pyknosis, as well as necrosis. Furthermore, cellular infiltrate was present in this group, but at a lower ratio than in the derivative **2** in the four groups (Fig. 10 (Liver A-F)).

3.4.2. Spleen

The structure of the spleen in the control group was characterized by well-defined white and red pulp with continuous trabeculae through all tissues encountered by the capsule. The whitish pulp contained lymphoid follicles as well. With the presence of trabeculae, Groups **III & VI** provided a similar definition. White pulp also has a consistent marginal zone and core.

The negative control group had the most splenic tissue damage, as evidenced by disordered white and red pulp and the presence of tachyzoites. The compound **2** group exhibited large, blocked blood arteries. Furthermore, the limits between white pulp and red pulp regions were not noticed, which was critical to the lowest extent of this treatment on splenic tissue.

Increase in the number of lymphoid follicles in the compound **4** group, underlining the importance of this therapy at this phase with the identification of the capsule around the spleen. In comparison to earlier studies, the alienated structure of group **VI** reflects the efficacy of the investigated compound **5** to the splenic tissue in similar action of antibiotic treatment.

The compound **5** group had to have an increase in lymphoid follicles, highlighting the significance of this treatment at this stage with the identification of the capsule around the spleen. In comparison to previous studies, the alienated configuration of group **VI** tends to reflect the efficacy of the derivative **5** to splenic tissue in an antibiotic-like action (Fig. 10 (Spleen A-F)).

3.4.3. Brain

Microscopic examination of H & E-stained cerebral cortex slices from the frontal region of the control group revealed the well-known normal cytoarchitecture of the cerebral cortex. Neurons, particularly pyramidal and granule cells, as well as neuroglial cells, are abundant within these layers. Significant multifocal histological abnormalities, culminating in a massive cerebral infract, were found when the infected group was examined.

In comparison to the previous findings, the treated groups (**IV** & **V**) had better histology and fewer vacuoles and small-disconnected brain foci. Besides that, tachyzoites were detected in group **IV**. Normal neuron architecture, with large vesicular nuclei in the center with one or more nucleoli and peripheral dispersion of Nissl granules were recorded indicating the influence of the ionic liquid **5** treatment versus antibiotic treatment (Fig. 10 (Brain A-F)).

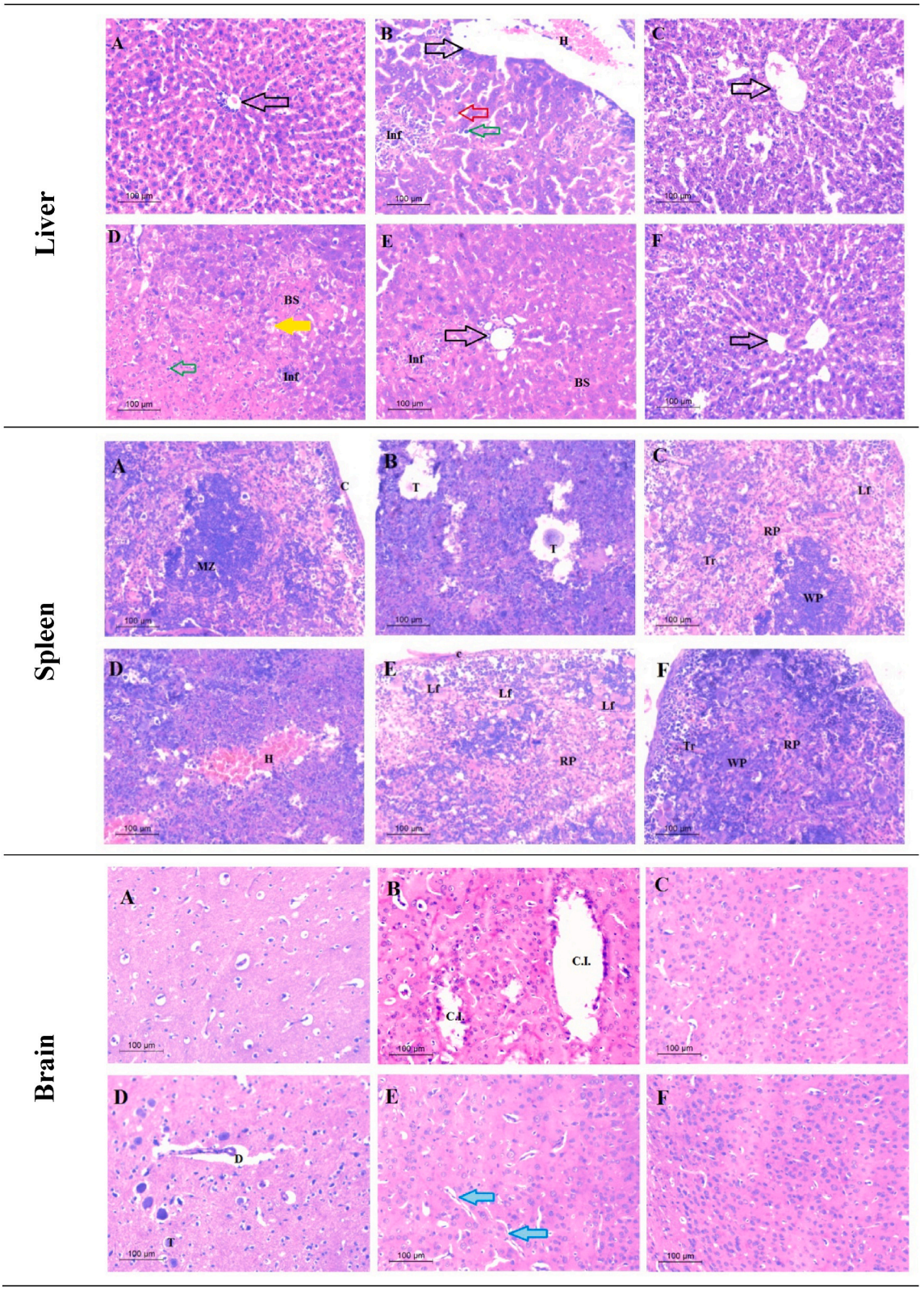

(caption on next page)

Fig. 10. A photomicrograph illustrates several H&E-stained tissue specimens from the liver spleen, and cerebrum. (**A**): control group; (**B**): infected group; (**C**): antibiotic Treated group; (**D**): compound **2** treated group; (**E**): compound **5** treated group; (**F**): compound **3** treated group magnification ×100. Where Black arrows central vein, Yellow arrow vacuolated hepatocyte, Inf cellular infiltrate, BS blood sinusoids, H hemorrhage, Green arrows Kupffer cells, T tachyzoites, MZ marginal zone, RP red Pulp, C capsule, Tr trabeculae, WP white pulp, L lymphoid follicle, C.I. cerebral infract, D degeneration, Blue arrow irregular body of neurons. (For interpretation of the references to colour in this figure legend, the reader is referred to the Web version of this article.)

4. Conclusion

Focused bis-pyridinium based-ionic liquids were successfully synthesized through the quaternization of the selected 1,2-di(pyridin-4-yl)ethane followed by metathetical anion exchange. The synthesized pyridinium derivatives were fully characterized using various NMR-spectroscopic techniques including ^{1}H, ^{13}C, ^{11}B, ^{31}P and ^{19}F NMR. The current available treatments for *Toxoplasma gondii* infection are restricted, besides that possess side effects and the spread of drug-resistant *T. gondii* strains. Consequently, a new anti-*Toxoplasma* drug should be available, therefore we emphasized novel alternatives, and well tolerated compounds. The investigated dicationic pyridinium derivatives exhibited a great reduction in *T. gondii* tachyzoites count in various organs compared to pyrimethamine (the known available drugs for toxoplasmosis). However, more drug doses need to be tested with further molecular and immunological studies are needed before testing the synthesized drugs in clinical studies.

Author contribution statement

Esraa Abdelhamid Moneer, Basant A. Bakr, Sara H. Akl, Yahya H. Shahin, Bassma H. Elwakil, Mohamed Hagar, Keshav Raj Paudel, Ateyatallah Aljuhani, Mohamed Reda Aouad; Nadjet Rezki: Conceived and designed the experiments; Performed the experiments; Analyzed and interpreted the data; Contributed reagents, materials, analysis tools or data; Wrote the paper.

Funding statement

This research did not receive any specific grant from funding agencies in the public, commercial, or not-for-profit sectors.

Data availability statement

Data will be made available on request.

Additional information

Supplementary content related to this article has been published online at [URL].

Declaration of competing interest

The authors declare that they have no known competing financial interests or personal relationships that could have appeared to influence the work reported in this paper.

Appendix A. Supplementary data

Supplementary data to this article can be found online at https://doi.org/10.1016/j.heliyon.2023.e15431.

References

[1] Lei Z., B. Chen, Y.-M. Koo, D.R. MacFarlane, ACS Publications, 2017, p. 6633-6635.
[2] S.K. Singh, A.W. Savoy, J. Mol. Liq. 297 (2020), 112038.
[3] R. Singh, A. Rasool, Br. J. Res. 6 (2018) 45.
[4] K.S. Egorova, E.G. Gordeev, V.P. Ananikov, Chem. Rev. 117 (2017) 7132.
[5] J.M. Gomes, S.S. Silva, R.L. Reis, Chem. Soc. Rev. 48 (2019) 4317.
[6] M. Ding, Y.-S. Zha, J. Zhang, S.-S. Wang, Colloids Surf. A Physicochem. Eng. Asp. 298 (2007) 201.
[7] S. Steudte, S. Bemowsky, M. Mahrova, U. Bottin-Weber, E. Tojo-Suarez, P. Stepnowski, et al., Toxicity and biodegradability of dicationic ionic liquids, RSC Adv. 4 (10) (2014) 5198–5205.
[8] T. Payagala, J. Huang, Z.S. Breitbach, P.S. Sharma, D.W. Armstrong, Chem. Mater. 19 (2007) 5848.
[9] P.S. Sharma, T. Payagala, E. Wanigasekara, A.B. Wijeratne, J. Huang, D.W. Armstrong, Chem. Mater. 20 (2008) 4182.
[10] A. Balducci, Ionic Liquids in Lithium-Ion Batteries. Ionic Liquids II, 2018, pp. 1–27.
[11] M.J. Earle, K.R. Seddon, Pure Appl. Chem. 72 (2000) 1391.
[12] N.V. Plechkova, K.R. Seddon, Chem. Soc. Rev. 37 (2008) 123.
[13] R.A.M. de Barros, A.C. Torrecilhas, M.A.M. Marciano, M.L. Mazuz, V.L. Pereira-Chioccola, B. Fux, Acta Trop. (2022), 106432.
[14] A. Oweimrin, Toxoplasma Gondii: Antibody Prevalence and Risk Factors in CU Boulder Students, 2018.

[15] F. Nogareda, Y. Le Strat, I. Villena, H. De Valk, V. Goulet, Epidemiol. Infect. 142 (2014) 1661.
[16] J. Dubey, F. Murata, C. Cerqueira-Cézar, O. Kwok, I. Villena, Parasitology 148 (2021) 1406.
[17] B.J. Bogitsh, C.E. Carter, T.N. Oeltmann, Human Parasitology, Academic Press, 2018.
[18] R.P.B. de Melo, F.S. Wanderley, W.J.N. Porto, C.d.M. Pedrosa, C.M. Hamilton, M.H.G.S. de Oliveira, M. Ribeiro-Andrade, R.C.d.S. Rêgo, F. Katzer, R.A. Mota, Parasitol. Res. 119 (2020) 2727.
[19] R.A. da Silva Sanfelice, T.F. Silva, F. Tomiotto-Pellissier, B.T. da Silva Bortoleti, D. Lazarin-Bidóia, S. Scandorieiro, G. Nakazato, L.D. de Barros, J.L. Garcia, W. A. Verri, Microb. Infect. 24 (2022), 104971.
[20] A.C. Anderson, Targeting DHFR in parasitic protozoa, Drug Discov. Today 10 (2) (2005) 121–128.
[21] D.G. Waller, A. Sampson, A. Hitchings, Medical Pharmacology and Therapeutics E-Book, Elsevier Health Sciences, 2021.
[22] N. Rezki, M. Messali, S.A. Al-Sodies, A. Naqvi, S.K. Bardaweel, F.F. Al-blewi, M.R. Aouad, H. El Sayed, J. Mol. Liq. 265 (2018) 428.
[23] N. Rezki, S.A. Al-Sodies, H.E. Ahmed, S. Ihmaid, M. Messali, S. Ahmed, M.R. Aouad, J. Mol. Liq. 284 (2019) 431.
[24] S. Al-Sodies, N. Rezki, F.F. Albelwi, M. Messali, M.R. Aouad, S.K. Bardaweel, M. Hagar, Int. J. Mol. Sci. 22 (2021), 10487.
[25] S.A. Al-Sodies, M.R. Aouad, S. Ihmaid, A. Aljuhani, M. Messali, I. Ali, N. Rezki, J. Mol. Struct. 1207 (2020), 127756.
[26] T. Mosmann, Rapid colorimetric assay for cellular growth and survival: application to proliferation and cytotoxicity assays, J. Immunol. Methods 65 (1–2) (1983) 55–63.
[27] S. Romand, M. Pudney, F. Derouin, In vitro and in vivo activities of the hydroxy naphthoquinone atovaquone alone or combined with pyrimethamine, sulfadiazine, clarithromycin, or minocycline against *Toxoplasma gondii*, Antimicrob. Agents Chemother. 37 (11) (1993) 2371–2378.
[28] J.-H. Jiang, C.-M. Jin, Y.-C. Kim, et al., Anti-toxoplasmosis effects of oleuropein isolated from *Fraxinus rhychophylla*, Biol. Pharm. Bull. 31 (12) (2008) 2273–2276.
[29] M. Jafari, Z. Lorigooini, S. Kheiri, K.M. Naeini, Anti-toxoplasma effect of hydroalchohlic extract of *Terminalia chebula* retz in cell culture and murine model, Iran. J. Parasitol. 16 (4) (2021) 631.
[30] N.A.E. Hagras, N.M.F.H. Mogahed, E. Sheta, A.A.E. Darwish, M.A. El-Hawary, M.T. Hamed, B.H. Elwakil, The powerful synergistic effect of spiramycin/propolis loaded chitosan/alginate nanoparticles on acute murine toxoplasmosis, PLoS Neglected Trop. Dis. 16 (3) (2022), e0010268.
[31] A. Thiptara, W. Kongkaew, U. Bilmad, T. Bhumibhamon, S. Anan, Ann. N. Y. Acad. Sci. 1081 (2006) 336.
[32] L.A. El-Zawawy, D. El-Said, S.F. Mossallam, H.S. Ramadan, S.S. Younis, Triclosan and triclosan-loaded liposomal nanoparticles in the treatment of acute experimental toxoplasmosis, Exp. Parasitol. 149 (2015) 54–64.
[33] M.L.d.O. Penido, D.L. Nelson, L.Q. Vieira, P.M.Z. Coelho, Mem. Inst. Oswaldo Cruz 89 (1994) 595.
[34] T.M. Almutairi, N. Rezki, M.R. Aouad, M. Hagar, B.A. Bakr, M.T. Hamed, M.K. Hassen, B.H. Elwakil, E.A. Moneer, Molecules 27 (2022) 2246.
[35] W.D. Wilson Francesconi, F.A. Tanious, J.E. Hall, B.C. Bender, R.R. Tidwell, D. McCurdy, D.W. Boykin, J. Med. Chem. 42 (1999) 2260.
[36] D.A. Molina, G.A. Ramos, A. Zamora-Vélez, G.M. Gallego-López, C. Rocha-Roa, J.E. Gómez-Marin, E. Cortes, Int. J. Parasitol.: Drugs Drug Resist. 16 (2021) 129.
[37] A.T. Hopper, A. Brockman, A. Wise, J. Gould, J. Barks, J.B. Radke, L.D. Sibley, Y. Zou, S. Thomas, J. Med. Chem. 62 (2019) 1562.